Electronic Supplementary Material (ESI) for Journal of Materials Chemistry A.

Insights into the Electronic Structure of Fe Penta-Coordinated Complexes. Spectroscopic Examination and Electrochemical Analysis for the Oxygen Reduction and Oxygen Evolution Reactions.

César Zúñiga Loyola[a], Gabriel Abarca[b], Soledad Ureta-Zañartu[a], Carolina Aliaga[a], Jose Zagal[a], Moulay Tahar Sougrati[c], Frédéric Jaouen[c], Walter Orellana[d], Federico Tasca[a*]

[a] Facultad de Química y Biología, Universidad de Santiago de Chile, Santiago, Chile.

[b] Universidad Bernardo O'Higgins, Centro Integrativo de Biología y Química Aplicada, Santiago Chile.

[c] ICGM, Univ. Montpellier, CNRS, ENSCM, Montpellier, France

[d] Departamento de Ciencias Físicas, Universidad Andrés Bello, Sazié 2212, 837-0136 Santiago, Chile.

*Corresponding author: Federico.tasca@usach.cl

Table S1. Mössbauer parameter determined for FePc-Py-CNT and assignment to Fe species (*)

Catalyst	Signal	δ_{Iso} (mm/s)	ΔE_Q (mm/s)	FWHM (mm/s)	Area (%)	Possible assignment
Doublet D_a	**a**	**0.23 (±0.04)**	**0.39 (±0.06)**	**0.28 (±0.07)**	**0.47 (±0.18)**	O-Fe(III)Pc-N or N-Fe(II)Pc-N
Doublet D_b	**b**	**0.22 (±0.03)**	**1.04 (±0.09)**	**0.45 (±0.12)**	**0.35 (±0.11)**	O-Fe(III)Pc/C
Doublet D_c	**c**	**0.39 (±0.08)**	**0.54 (±0.23)**	**0.28 (±0.07)**	**0.18 (±0.08)**	O-Fe(III)Pc-N or N-Fe(II)Pc-N

(*) Errors are given between parentheses.

Table S2. Binding energy for FePc-CNT and FePc-Py-CNT before and after treatment with O_2.

	Before exposure to O_2		**After exposure to O_2**	
	Binding energy (eV)			
Compound	**Binding energy (eV) FePc-CNT**	**FePc-Py-CNT**	**Binding energy (eV) FePc-CNT**	**Binding energy (eV) FePc-Py-CNT**
Fe^0	-	-	-	707.4
Fe^{2+} (oct)	708.5	708.7	708.7	708.9
Fe^{3+} (oct)	709.7	709.8	710.3	710.2
Fe^{3+} (td)	712.0	711.7	713.6	711.9
Fe^{2+} (sat)	714.9	714.1	715.2	714.1
Fe^{3+} (sat)	718.5	718.7	718.2	718.8
Fe^{2+}/ Fe^{3+}	0.42	0.33	0.52	0.57

Table S3. XPS experimental parameter for FePc-CNT before and after exposure to O_2.

Compound	Before treatment with O_2		After treatment with O_2	
	FWHM* FePc-CNT	Atomic (%) FePc-CNT	FWHM FePc-CNT	Atomic (%) FePc-CNT
Fe^0	-	-	-	-
$Fe^{2+}_{(oct)}$	1.7	23.34	1.5	23.25
$Fe^{3+}_{(oct)}$	2.8	47.19	2.1	36.77
$Fe^{3+}_{(td)}$	2.8	17.14	2.2	19.67
$Fe^{2+}_{(sat)}$	2.7	6.06	3.1	11.39
$Fe^{3+}_{(sat)}$	2.7	6.26	3.5	8.93

**FWHM is the full width at half maximum.*

Table S4. XPS experimental parameter for FePc-Py-CNT before and after exposure to O_2.

	Before treatment with O_2		**After treatment with O_2**	
Compound	**FWHM FePc-Py-CNT**	**Atomic (%) FePc-Py-CNT**	**FWHM FePc-Py-CNT**	**Atomic (%) FePc-Py-CNT**
Fe^0	-	-	1.6	2.18
Fe^{2+} (oct)	1.7	18.87	1.6	18.87
Fe^{3+} (oct)	1.7	40.55	1.8	36.55
Fe^{3+} (td)	1.9	23.14	1.9	19.14
Fe^{2+} (sat)	2.8	6.44	3.2	15.25
Fe^{3+} (sat)	3.4	10.99	3.5	8.01

**FWHM is the full width at half maximum.*

Table S5. Bifunctional performance for various bifunctional electrocatalyst for ORR and OER.

Catalyst	E_{10} (V vs. RHE)	$E_{1/2}$ ORR (V vs. RHE)	ΔE (V vs. RHE)	Tafel slope (V dec^{-1})		References
				ORR	OER	
FePc-Py-CNT	~1.615	0.935	0.680	-0.022	0.214	This work
FeCoOOH-NF⊥3D-FeNC	1.46	0.855	0.605	-0.070	0.054	[10]
Ex-FeN-MC	1.480	0.850	0.630	-	0.047	[11]
S, N-Fe/N/CNT	1.600	0.850	0.750	-	0.082	[12]
FePc-GO	1.650	0.890	0.760	-	0.112	[13]
1@ZIF-67	1.646	0.850	0.796	-0.056	0.106	[14]
FeNC	1.550	0.720	0.830	-		[15]
CoPc-GO	1.600	0.760	0.840	-	0.083	[13]
Mn/Co-N-C	1.660	0.800	0.860	-0.077	0.145	[16]
Fe-N_x-C	1.830	0.910	0.920	-0.069	0.243	[17]
2/CNT	1.710	0.760	0.95	-0.043	0.072	[18]
Ir/C 20 wt% (Vulcan)	1.095	0.660	1.095	-0.141	0.105	[19]
RuO_2	1.640	0.540	1.100	-	-	[20]
Pt/C 20 wt% (Vulcan)	> 2.000	0.810	>1.2	-0.085	0.155	[21]
IrO_2	1.700	0.380	1.320	-	-	[20]
MWCNT-20@B	1.910	0.560	1.350	-	-	[22]

Table S6. EIS parameters for the ORR at CNT/GC, Py-CNT/GC and FePc-Py-CNT/GC electrodes in deaerated and O_2 saturated 0.1 M KOH.

Electrode	F_R	E/V vs. RHE	Deaerated R_uC_{dl} circuit		O_2 saturated, $R_u(R_FC_{dl})$ circuit		
			R_u /Ω cm^2	C_{dl} /μF cm^{-2}	R_u /Ω cm^2	R_F /kΩ cm^2	C_{dl} /μF cm^{-2}
CNT/GC	6.13	0.88	129	62.6	134	4.82	655
Py-CNT/GC	1.10	0.88	133	100	136	105	84.0
FePc-Py-CNT/GC	6.13	0.88	90.5	737	98	15.6	873
CNT/GC	6.13	0.78	129	717	129	Error > 10%	717
Py-CNT/GC	1.10	0.78	133	117	133	Error > 10%	117
FePc-Py-CNT/GC	6.13	0.78	94.4	1140	94.3	Error > 10%	1140

Table S7. EIS parameters for FePc-Py-CNT/GC electrode (8.6×10^{-8} mol Fe cm^{-2}; F_R = 17.5**)** according to the[R(RC)] equivalent circuit.

E / V vs. RHE	R_u / Ω cm^2	R_F / kΩ cm^2	C_{dl} /mF cm^{-2}
0.78	8.59	4.66	5.13
1.18	8.8	6.99	2.03
1.38	10.9	2.44	2.18
1.43	10	0.594	13.8

Table S8. EIS parameters at 1.38 V vs. RHE for the three kinds of electrodes.

Electrode	F_R	R_u / Ω cm^2	R_F /kΩ cm^2	C_{dl} /mF cm^{-2}
CNT/GC	4.58	6.79	1.13	8.34
Py-CNT/GC	1.66	10.6	8.09	1.66
FePc-Py-CNT/GC	6.58	5.59	0.64	14

Table S9. Equilibrium distance between Fe atom and its first-neighbours' atoms in FePc-CNT. (Fe) is the vertical displacement of the Fe atom respect to the FePc plane once the O_2 molecule is adsorbed.

Distance (Å)	FePc-CNT (m=2)	O_2-FePc-CNT (m=0)
Fe-N1	1.931	1.946
Fe-N2	1.931	1.933
Fe-N3	1.93	1.933
Fe-N4	1.932	1.947
Fe-O	-	1.774
O-O	-	1.286
Fe-C	2.948	3.156
Δz(Fe)	0	0.19

The O_2 binding energy is calculated to be of -0.809 eV. We note that the O-O bond distance increases 3.6% with respect to gas phase O_2.

Table S10. Equilibrium distances between Fe atom and their first-neighbours' atoms in FePc-Py-CNT. (Fe) is the vertical displacement of the Fe atom respect to the FePc plane once the O_2 molecule is adsorbed.

Distance (Å)	FePc-Py-CNT (m=2)	O_2-FePc-Py-CNT (m=1)
Fe-N1	1.936	1.959
Fe-N2	1.935	1.958
Fe-N3	1.935	1.942
Fe-N4	1.936	1.943
Fe-N5	1.887	2.09
Fe-O	-	1.832
O-O	-	1.292
Δz (Fe)	-0.17	0.01

The O_2 binding energy is calculated to be of -0.758 eV. We note that the O-O bond distance increases 4.1% with respect to gas phase O_2.

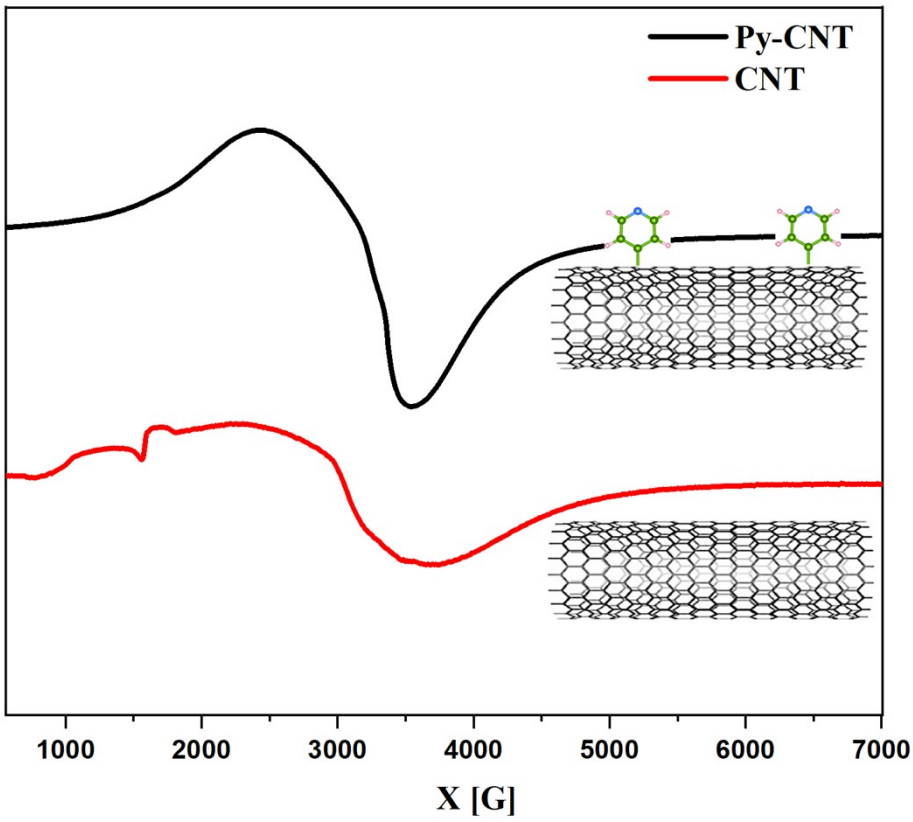

Figure S1. EPR spectrum of Py-CNT and CNT.

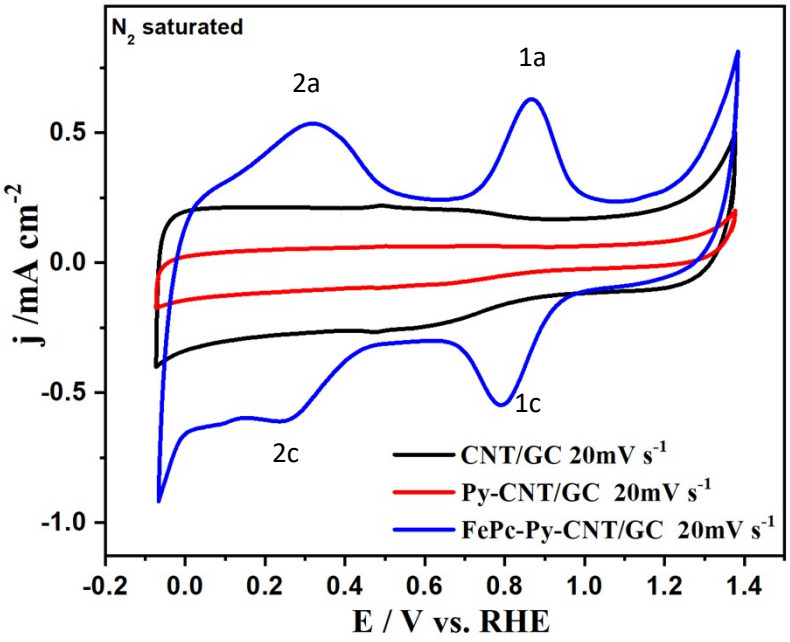

Figure S2. Cyclic voltammetry at 20 mV s^{-1} in deaerated 0.1 M KOH using CNT/GC, Py-CNT/GC and FePc-Py-CNT/GC electrodes.

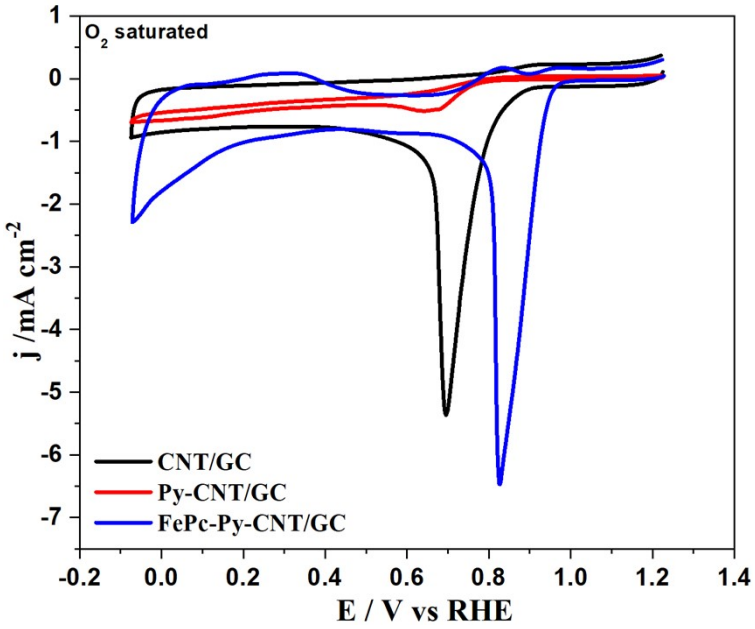

Figure S3. Cyclic voltammetry at 20 mV s^{-1} in O_2 saturated 0.1 M KOH for CNT/GC, Py-CNT/GC and FePc-Py-CNT/GC electrodes.

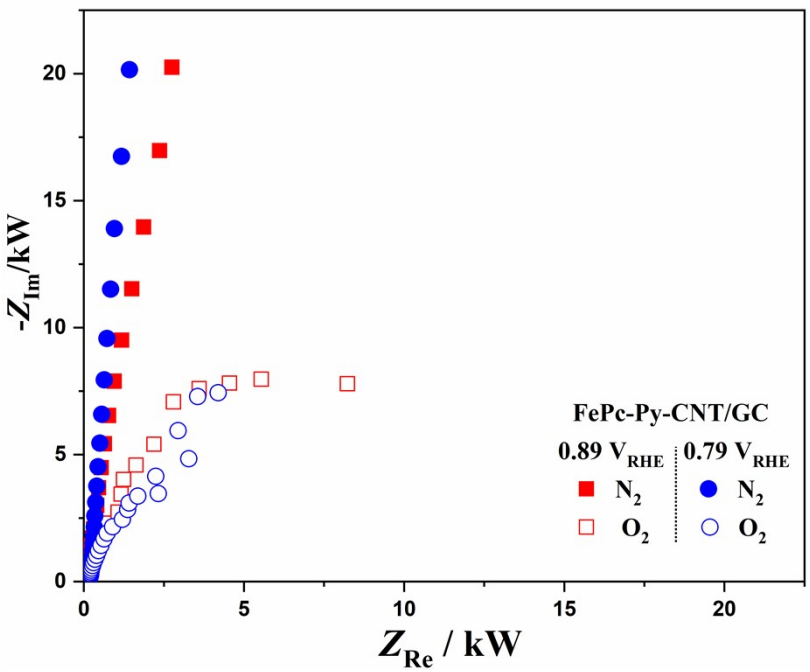

Figure S4. Nyquist plots at 0.89 V (squares) and 0.79 V (circles) vs. RHE under deaerated (closed symbols) and O_2 saturated (opened symbols) in 0.1 M KOH solution using FePc-Py-CNT/GC electrode.

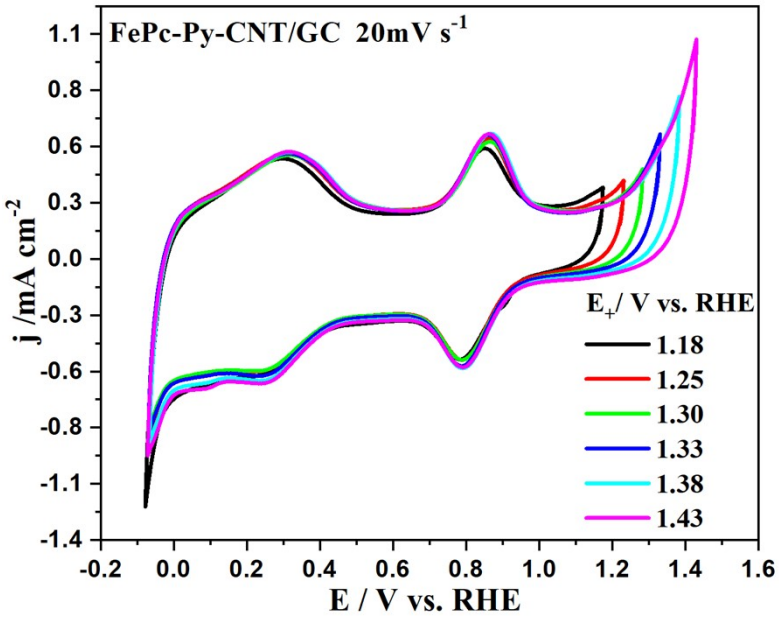

Figure S5. Cyclic voltammetry at 20 mV s^{-1} in N_2 to different potential ranges for FePc-Py-CNT/GC in 0.1M KOH.

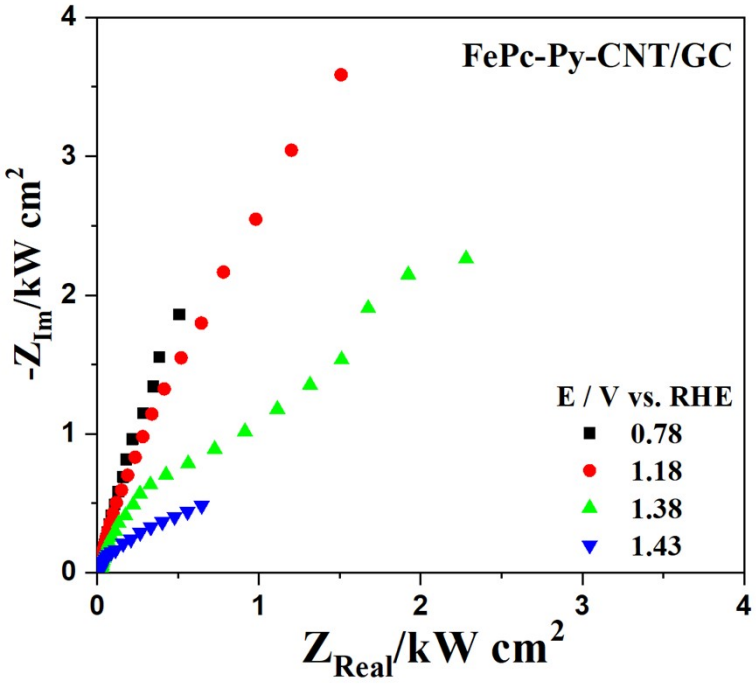

Figure S6. Nyquist plots at 0.78, 1.18, 1.38, and 1.43 V vs. RHE in deaerated 0.1M KOH using FePc-Py-CNT/GC electrode.

References

1 C. A. Melendres, *J. Phys. Chem.*, 1980, **84**, 1936–1939.

2 U. I. Koslowski, I. Abs-Wurmbach, S. Fiechter and P. Bogdanoff, *J. Phys. Chem. C*, 2008, **112**, 15356–15366.

3 U. I. Kramm, M. Lefèvre, N. Larouche, D. Schmeisser and J. P. Dodelet, *J. Am. Chem. Soc.*, 2014, **136**, 978–985.

4 D. A. Summerville, I. A. Cohen, K. Hatano and W. R. Scheidt, *Inorg. Chem.*, 1978, **17**, 2906–2910.

5 R. Taube, *Pure Appl. Chem.*, 1974, **38**, 427–438.

6 L. Ni, C. Gallenkamp, S. Paul, M. Kübler, P. Theis, S. Chabbra, K. Hofmann, E. Bill, A. Schnegg, B. Albert, V. Krewald and U. I. Kramm, *Adv. Energy Sustain. Res.*, 2021, **2**, 2000064.

7 G. R. HOY, *Industrial Applications of the Mössbauer Effect*, Springer Netherlands, Notfolk, Virginia, 1st edn., 2002.

8 U. I. Kramm, J. Herranz, N. Larouche, T. M. Arruda, M. Lefèvre, F. Jaouen, P. Bogdanoff, S. Fiechter, I. Abs-Wurmbach, S. Mukerjee and J.-P. Dodelet, *Phys. Chem. Chem. Phys.*, 2012, **14**, 11673–11688.

9 T. C. G. N.N. Greenwood, in *Methods in molecular biology (Clifton, N.J.)*, 2011, vol. 766, pp. 221–235.

10 S. Ibraheem, S. Chen, J. Li, Q. Wang and Z. Wei, *J. Mater. Chem. A*, 2019, **7**, 9497–9502.

11 R. Akram, M. A. Ud Din, S. U. Dar, A. Arshad, W. Liu, Z. Wu and D. Wu, *Nanoscale*, 2018, **10**, 5658–5666.

12 P. Chen, T. Zhou, L. Xing, K. Xu, Y. Tong, H. Xie, L. Zhang, W. Yan, W. Chu, C. Wu and Y. Xie, *Angew. Chemie - Int. Ed.*, 2017, **56**, 610–614.

13 W. Wan, C. A. Triana, J. Lan, J. Li, C. S. Allen, Y. Zhao, M. Iannuzzi and G. R. Patzke, *ACS Nano*, 2020, **14**, 13279–13293.

14 Z. Liang, H. Guo, G. Zhou, K. Guo, B. Wang, H. Lei, W. Zhang, H. Zheng, U. P. Apfel and R. Cao, *Angew. Chemie - Int. Ed.*, 2021, 1–6.

15 K. Mamtani, D. Jain, A. C. Co and U. S. Ozkan, *Energy and Fuels*, 2017, **31**, 6541–6547.

16 L. Wei, L. Qiu, Y. Liu, J. Zhang, D. Yuan and L. Wang, *ACS Sustain. Chem. Eng.*, 2019, **7**, 14180–14188.

17 J. Han, X. Meng, L. Lu, J. Bian, Z. Li and C. Sun, *Adv. Funct. Mater.*, 2019, **29**, 1808872.

18 H. Qin, Y. Wang, B. Wang, X. Duan, H. Lei, X. Zhang, H. Zheng, W. Zhang and R. Cao, *J. Energy Chem.*, 2021, **53**, 77–81.

19 D. Zhou, Z. Cai, X. Lei, W. Tian, Y. Bi, Y. Jia, N. Han, T. Gao, Q. Zhang, Y. Kuang, J. Pan, X. Sun and X. Duan, *Adv. Energy Mater.*, 2018, **8**, 1–7.

20 R. A. Rincón, J. Masa, S. Mehrpour, F. Tietz and W. Schuhmann, *Chem. Commun.*, 2014, **50**, 14760–14762.

21 X. Xing, R. Liu, K. Cao, U. Kaiser, G. Zhang and C. Streb, *ACS Appl. Mater. Interfaces*, 2018, **10**, 44511–44517.

22 Y. Cheng, Y. Tian, X. Fan, J. Liu and C. Yan, *Electrochim. Acta*, 2014, **143**, 291–296.